Temporally chimeric mice reveal flexibility of circadian period-setting in the suprachiasmatic nucleus

Nicola J. Smyllie[a], Johanna E. Chesham[a], Ryan Hamnett[a], Elizabeth S. Maywood[a], and Michael H. Hastings[a,1]

[a]Division of Neurobiology, Medical Research Council Laboratory of Molecular Biology, Cambridge, CB2 0QH United Kingdom

The suprachiasmatic nucleus (SCN) is the master circadian clock controlling daily behavior in mammals. It consists of a heterogeneous network of neurons, in which cell-autonomous molecular feedback loops determine the period and amplitude of circadian oscillations of individual cells. In contrast, circuit-level properties of coherence, synchrony, and ensemble period are determined by intercellular signals and are embodied in a circadian wave of gene expression that progresses daily across the SCN. How cell-autonomous and circuit-level mechanisms interact in timekeeping is poorly understood. To explore this interaction, we used intersectional genetics to create temporally chimeric mice with SCN containing dopamine 1a receptor (Drd1a) cells with an intrinsic period of 24 h alongside non-Drd1a cells with 20-h clocks. Recording of circadian behavior in vivo alongside cellular molecular pacemaking in SCN slices in vitro demonstrated that such chimeric circuits form robust and resilient circadian clocks. It also showed that the computation of ensemble period is nonlinear. Moreover, the chimeric circuit sustained a wave of gene expression comparable to that of nonchimeric SCN, demonstrating that this circuit-level property is independent of differences in cell-intrinsic periods. The relative dominance of 24-h Drd1a and 20-h non-Drd1a neurons in setting ensemble period could be switched by exposure to resonant or nonresonant 24-h or 20-h lighting cycles. The chimeric circuit therefore reveals unanticipated principles of circuit-level operation underlying the emergent plasticity, resilience, and robustness of the SCN clock. The spontaneous and light-driven flexibility of period observed in chimeric mice provides a new perspective on the concept of SCN pacemaker cells.

period | entrainment | neuropeptide | circuit | oscillator

Daily rhythms of behavior and physiology adapt organisms to the solar cycle. In mammals, these rhythms are coordinated by a central circadian pacemaker: the suprachiasmatic nucleus (SCN) of the hypothalamus (1). The SCN consists of 10,000 neurons that work together to ensure that rhythms are tuned appropriately to anticipate day and night. Circadian dysfunction is increasingly linked to a variety of psychological and metabolic disorders (2). The principal subdivisions of the SCN are the shell, characterized by neurons expressing arginine vasopressin (AVP), and the retinorecipient core, containing vasoactive intestinal peptide (VIP) and gastrin-releasing peptide (GRP) neurons. The core mediates entrainment to light after birth (3), whereas neurons expressing the dopamine 1a receptor (Drd1a) mediate transplacental dopaminergic entrainment of the SCN in utero (4). Drd1a cells are, therefore, a functionally distinct subpopulation that spans elements of both core and shell.

Timekeeping in individual SCN neurons involves a molecular clockwork based on a transcriptional–translational feedback loop (TTFL) whereby PERIOD and CRYPTOCHROME proteins inhibit their own transactivation by CLOCK/BMAL1 heterodimers (5). Almost all of the cells in the body also have this TTFL, but in the absence of SCN input, the amplitude and synchrony of peripheral circadian oscillations are lost. A defining feature of the SCN, therefore, is its intrinsic ability to sustain stable, high-amplitude circadian rhythms (6). Importantly, this is dependent on neuropeptide-mediated interneuronal communication (7–9). This property is embodied in an emergent spatiotemporal wave of gene expression that progresses

daily across the SCN, observed in real-time recordings of Per- and Cry-driven bioluminescence in SCN slices (8, 10). The principles that underpin the relationship between cell-autonomous and circuit-level properties are unknown.

To explore these principles, we sought to modulate circadian function in a subset of neurons in the SCN and examine the consequences circuit-wide. We selected a GENSAT (Gene Expression in the Nervous System Atlas) transgenic mouse line that expressed Drd1a promoter-driven Cre recombinase (Cre) with very high expression in the SCN and atypically low expression in other brain areas (11). We used Cre-mediated deletion of the casein kinase 1 epsilon ($CK1\varepsilon$) Tau mutation that accelerates the TTFL (12) to create temporally chimeric mice in which the SCN contained cells with contrasting cell-autonomous periods: 24 h (Tau-deleted) or 20 h (Tau-competent). Importantly, our approach kept intrinsic circadian timekeeping intact in all cells. This contrasts with studies that have selectively removed circadian function in a particular cell population through deletion or overexpression of a core clock gene (13–15). A major limitation of loss/overexpression of circadian transcription factors is that it not only confounds cell-autonomous timing but also compromises expression of neuropeptides that mediate intercellular signaling (14). This renders it difficult to dissociate contributions of cell-autonomous and intercellular mechanisms to circuit-level computations. We therefore considered our enzymatic modulation of cell-autonomous period to provide a valuable complementary perspective on SCN pacemaking. Having created chimeric mice, we could ask whether such a circuit is competent to generate circadian behavioral and molecular rhythms. If so, what is the emergent period? Do Drd1a cells dominate, or are multiple periodicities maintained? Does the altered distribution of

Significance

The suprachiasmatic nucleus (SCN) is the principal circadian clock of the mammalian brain. To function effectively, SCN neurons must operate as a synchronized circuit. How cell-autonomous and circuit-level circadian mechanisms interact to achieve this is unclear. Here, we used intersectional genetics to create temporally chimeric mice where both 24-h and 20-h clock neurons were present in the SCN, in different cell populations. The 24-h dopamine receptor-positive cells set the speed of the SCN, imposing their cell-autonomous 24-h period on all cells in the circuit. Exposure to a 20-h lighting cycle, however, inverted this dominance, reprograming the circuit to 20 h. These results show how robust circuit-level signaling underlies complex, nonlinear computations of circadian period that also exhibit a remarkable level of plasticity.

NEUROSCIENCE

cell-autonomous periods in the chimeric circuit affect other circuit-level properties, for example synchrony and generation of the spatiotemporal wave? Finally, what are the limits to the function of such a chimeric circuit? How plastic is it, and how might it be modulated?

Results

Circadian Behavior in Temporally Chimeric Mice. The activity of Cre across the brain of *Drd1a-Cre* mice was revealed by Cre-mediated constitutive expression of enhanced yellow fluorescent protein (EYFP) (*ROSA26-EYFP*) (16). Consistent with the GENSAT expression data, this generated strong fluorescence in the SCN (Fig. S1*A*), with varying levels in the olfactory bulb, amygdala, nucleus accumbens, and scattered striato-nigral neurons. Otherwise, fluorescence across the brain was at background levels. Neuropeptide immunofluorescence revealed that EYFP colocalized with a majority of AVP neurons and VIP neurons (Fig. S1 *B and C*). EYFP was almost entirely absent from GRP neurons. AVP, VIP, and GRP do not represent the entire SCN, and overall, two-thirds of SCN cells identified by DAPI stain expressed Cre (Fig. S1*B*). Thus, *Drd1a*-driven Cre expression is restricted to a neurochemically defined subset of SCN neurons incorporating elements of shell and core.

Drd1a-Cre, ROSA26-EYFP mice (*DCR*) were then crossed with mice carrying floxed $CK1\varepsilon^{Tau}$ alleles (12), along with the PER2:: LUCIFERASE bioluminescent reporter (17). Thus, in *DCR-CK1ε^{Tau}* mice, the SCN (and potentially other brain regions) should be a chimera of 24-h *Drd1a* cells alongside 20-h non-*Drd1a* cells. Deletion of *CK1ε* was confirmed by PCR (Fig. S1*I*). Importantly, neuropeptide expression was not significantly different in these animals compared with wild type (WT) (Fig. S1 *D and E*), indicating that neuropeptide-mediated signaling is likely to be intact in the chimeric SCN. Wheel-running behavior rhythms were monitored to assess the effect of temporal chimerism in vivo (Fig. 1*A*). DCR^+-$CK1\varepsilon^{WT}$ mice had well-organized activity patterns,

comparable to DCR⁻ animals (Fig. 1*C* and Table S1). Thus, expression of Cre itself did not affect behavior. As expected, the $CK1\varepsilon^{Tau}$ allele shortened the period by ca. 2 h per copy in DCR⁻ (*Tau*) mice. DCR^+ mice carrying $CK1\varepsilon^{Tau}$ alleles also exhibited organized free-running activity rhythms. Chimerism did not, therefore, compromise circadian control of behavior. Chimerism did, however, dramatically lengthen the period of wheel-running behavior compared with DCR⁻ animals (Fig. 1*C* and Table S1). This effect was not fully penetrant, and two principal phenotypes were apparent: The majority (9/15; 60%) had a period very close to 24 h—i.e., WT-like—consistent with a fully dominant effect of *Tau* deletion. We describe these animals as "Revertants." A subset of mice (5/15; 33%), which we refer to as "Non-Revertant," displayed a shorter period, consistent with their *Tau* genotype. This dichotomy is clear in the bimodal frequency plot (Fig. 1*D*). Interestingly, 1 out of fifteen displayed unstable behavioral rhythms (Fig. S2*A*).

The consequences of chimerism were reflected in entrained daily activity profiles of wheel running (Fig. S2 *B–E*). Revertant animals entrained to the light–dark (LD) cycle, with a clear onset of consolidated nocturnal activity (Fig. S2*D*), whereas entrainment to 24-h cycles was variable in Non-Revertant animals (Fig. S2*E*), similar to *Tau* mice. Thus, Revertants showed minimal activity in the light phase, comparable to WT, whereas *Tau* and some Non-Revertant mice failed to entrain, exhibiting significantly higher levels of photophase activity (Fig. S2*F*). Importantly, chimerism did not affect the overall duration of wheel-running (alpha), which was comparable across all genotypes in LD (Fig. S2*G*). This suggests that neuropeptide-mediated coupling of SCN subcircuits regulating evening and morning activity bouts was intact, in contrast to the disruptive effects of TTFL-based chimerism (14). In summary, targeted manipulation of the cell-autonomous period in *Drd1a* neurons did not compromise coherent timekeeping but did respecify the period of behavior in the majority of mice and, by inference, the period of the SCN circuit.
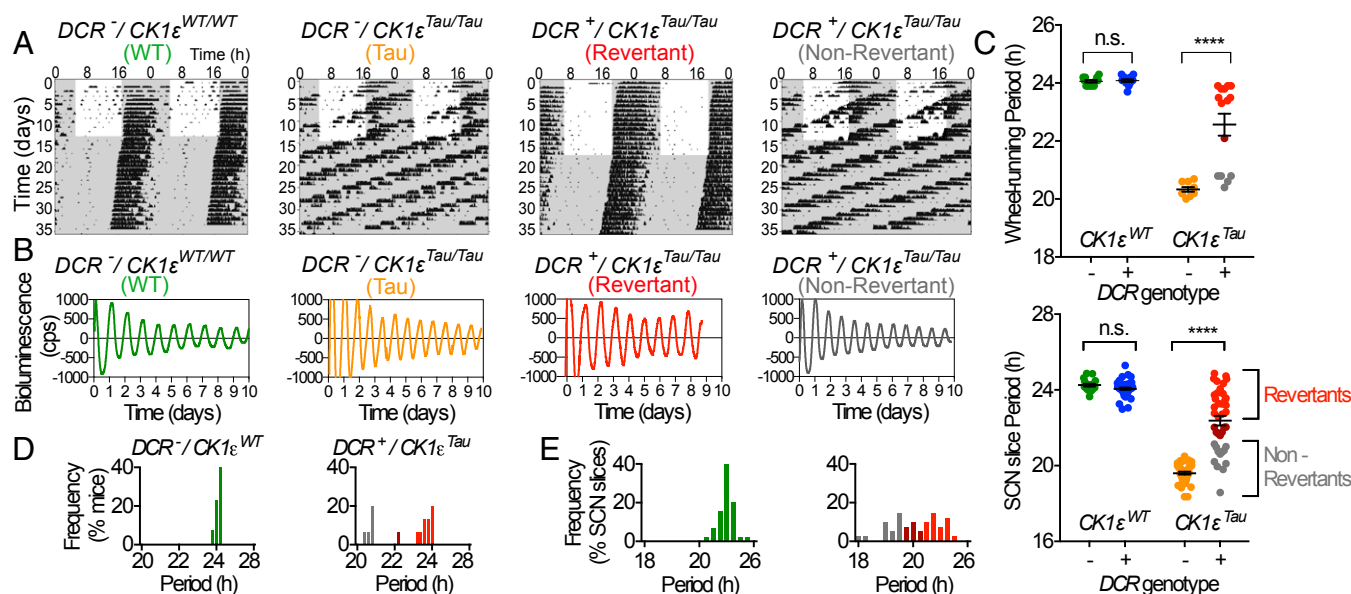

Fig. 1. Circadian period in temporally chimeric mice. (*A*) Representative double-plotted actograms from control $DCR^-/CK1\varepsilon^{WT}$ (green), mutant $DCR^-/CK1\varepsilon^{Tau}$ (orange), and temporally chimeric $DCR^+/CK1\varepsilon^{Tau}$ animals. Chimeric animals displayed a range of phenotypes, including Revertant (red) that phenocopied WT and Non-Revertant (gray) that phenocopied mutant *Tau* animals. White and gray backgrounds indicate lights on and off, respectively. (*B*) Representative PER2::LUC bioluminescence traces (de-trended) show circadian oscillations in SCN organotypic slices, where Revertant and Non-Revertant slices phenocopied WT and *Tau*, respectively. (*C*) Group data (mean ± SEM), across a $CK1\varepsilon^{Tau}$ mutant background, with (+) and without (−) *Drd1a-Cre* (*DCR*) for wheel-running (*n* > 6 per group) and SCN slices (*n* > 10 per group). Cre activity significantly lengthened the circadian period of behavior in the presence of $CK1\varepsilon^{Tau}$ (two-way ANOVA with Tukey's comparison, ****$P < 0.0001$). The period phenotype in the SCN matched that of behavior. Period was significantly lengthened in the chimeric SCN (Tukey's post hoc test following two-way ANOVA, n.s. $P > 0.05$, ****$P < 0.0001$). (*D*) Frequency distribution plots of the behavioral period in DCR^+ animals illustrate the broad multimodal spread in the CK1ε^{Tau} population compared with CK1ε^{WT}. (*E*) Frequency distribution for SCN slice circadian period.

Molecular Pacemaking in SCN of Temporally Chimeric Mice. PER2::LUC bioluminescence was monitored in organotypic SCN slices. The majority of chimeric SCNs exhibited very clear circadian cycles of bioluminescence (Fig. 1B). As with behavior, temporal chimerism did not destabilize circadian function of the SCN. It did, however, significantly lengthen the period compared with *Tau* SCN slices (Fig. 1C). Importantly, this effect was tissue-specific because a range of tissues that do not express *Drd1a-Cre* (cerebellum, liver, and lung) faithfully reported their *Tau* genotype, irrespective of Cre genotype (Fig. S3 and Table S2). Furthermore, the period of retinal explants remained ca. 20 h (Fig. S3F). Nevertheless, a dichotomy in chimeric SCN phenotype was again seen, with both Revertant and Non-Revertant SCNs at ratios comparable to those seen for behavior. A potential cause of the spectrum of the chimeric phenotype could be differing levels of Cre activity between animals, but we did not find clear evidence that this was the case. There were no detectable differences in the intensity or distribution of Cre-dependent EYFP expression (Fig. S1 F and G) or the copy number of Cre transgene between Revertant and Non-Revertant SCN (Fig. S1H). Moreover, assessment of *CK1ε* deletion in SCN genomic DNA did not reveal any obvious differences in the efficiency of deletion (Fig. S1 I and J). Paired measurements of period in wheel-running and SCN PER2::LUC oscillations from the same animal were highly correlated (Fig. S3G and Table S1): Mice identified as Revertants or Non-Revertants in vivo had SCNs of the corresponding phenotype (Fig. S3H). Thus, the ensemble SCN period was predictive, and likely the source, of chimeric behavior in vivo.

Seven of the 46 SCN slices had rhythms with multiple periods (Fig. S2 H and I) reminiscent of the single mouse from the wheel-running cohort that exhibited unstable behavioral rhythms (Fig. S2A). To investigate this further, we screened for animals that displayed multiple behavioral periods (Fig. S4). Eight "Mixed-period" animals showed behavior that switched back and forth between short (<21 h) and long (~24 h) periods (Fig. S4B), in contrast to Revertant and Non-Revertant mice, which displayed a very stable 24-h and 20-h period, respectively. Furthermore, this was reflected in PER2::LUC SCN rhythms. Peak-to-peak period varied greatly in SCNs from Mixed-period mice, whereas the period remained stable in *Tau* and Revertant SCN slices (Fig. S4C). This suggests that spontaneous plasticity of period-setting can occur in individual SCN networks and the direction of spontaneous change from long (Revertant) to short (Non-Revertant) cannot be explained by differences in Cre-mediated excision, which only causes short to long transitions.

Cell-Autonomous Circadian Pacemaking in Temporally Chimeric SCN. The variable effect of chimerism between animals raised the possibility that ensemble period is a stochastic property of the network. Tetrodotoxin (TTX), a disruptor of neuronal communication (8), was applied to SCN slices to observe whether on removal of TTX the circuit reassembled with the same phenotype (Fig. S5A). By monitoring PER2::LUC, it was clear that this was the case (Fig. S5 B–E). Thus, the Non-Revertant/Revertant nature of a chimeric SCN was a self-organizing, determinative property of each circuit.

To characterize the relationship between circuit-level and cell-autonomous circadian pacemaking, PER2::LUC rhythms were monitored by CCD in individual cells (Fig. S5 F–J) of SCNs treated with TTX. Before treatment, all Revertant and Non-Revertant SCNs, alongside corresponding WT and *Tau* controls, displayed tight, unimodal frequency distributions of period and phase, with steep cumulative frequency slopes (Fig. S6 A–E and Table S3). TTX increased the spread of cellular periods and relative phases for all genotypes, as disconnected cells expressed cell-autonomous properties. This reverted to the pretreatment configuration on TTX washout. Measures of cellular period and relative phase during TTX treatment confirmed temporal chimerism at the cell-autonomous level. For *DCR*⁻ control SCNs (both WT and *Tau*), the dispersals of
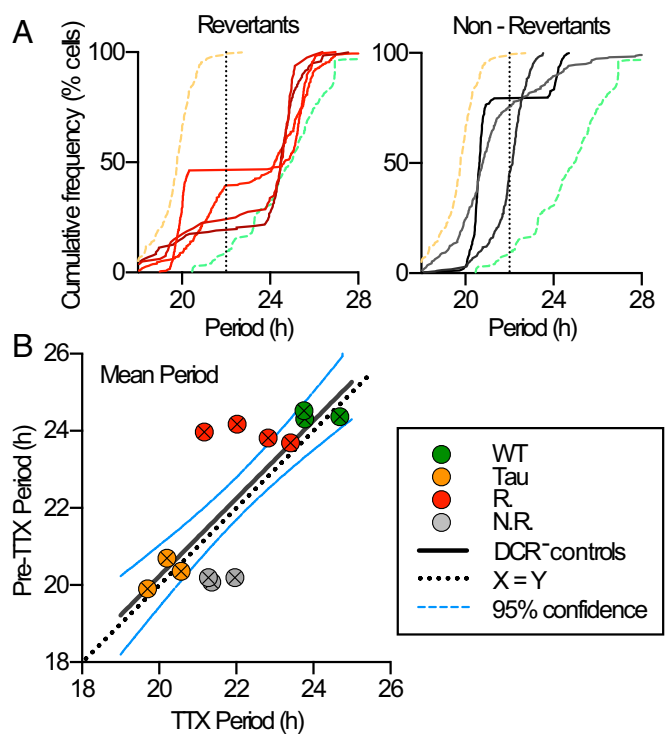

Fig. 2. Nonlinear computation of SCN period in temporally chimeric mice. (A) Cumulative frequency plots showing the distribution of circadian periods of neurons during treatment of SCN slices with TTX (1 μM). Revertant SCN slices (red traces; *Left* panel) show bimodal distribution, whereas Non-Revertant slices (gray traces; *Right* panel) display an even distribution from 20 h up to 24 h. For comparison, both graphs show average plots for *Tau* ($n = 3$, yellow dashed line) and WT slices ($n = 3$, green dashed line). The black dotted line indicates 22 h. Note the bimodal distribution of Revertant slice periods, on either side of the 22 h line. (B) Relationship between observed SCN ensemble period (Pre-TTX) and period predicted by distribution of cell-autonomous periods under TTX (mean of single-cell data, $n > 100$ cells per SCN and $n \geq 3$ SCN per group). Regression plot using data from control WT and *Tau* SCNs (solid line, $y = 1.008x + 0.73$) is not significantly different from line of equality (dotted). Note that the data from Revertant and Non-Revertant temporally chimeric mice fall off the control line. In addition, three of four Revertant and three of three Non-Revertant slices fall outside the 95% confidence intervals (blue dashed line), indicating nonlinear computation of the ensemble circadian period. The periods predicted from TTX data are longer than (Non-Revertant) or shorter than (Revertant SCN) those observed, although the predicted periods do not differ between the two phenotypic categories (Student's *t* test, $P = 0.23$).

cellular period and phase were symmetrical about the pre-TTX distribution, with no skewness (Fig. S6C). In four of six Revertant SCNs, however, cellular circadian periods under TTX became bimodal, showing two distinct plateaus in cumulative frequency plots (Fig. 2A and Table S3). One cell cluster remained at ca. 24 h, whereas a second emerged with a mean period of 20 h. In the remaining two Revertant SCNs, TTX produced a phase realignment with a bimodal distribution (Fig. S6B and Table S3). In the case of 20-h Non-Revertant SCNs, TTX again dispersed cellular period, and the distribution was asymmetrical with a larger proportion of cells expressing periods greater than 20 h: The cumulative frequency curves were right-shifted compared with *Tau* slices (Fig. 2A and Fig. S6E). Under TTX, therefore, both the Revertant and Non-Revertant SCNs contained a mix of short (putative *Tau*-competent) and long (*Tau*-deleted) period cells, but the Non-Revertant had relatively fewer cells with an autonomous period significantly longer than 20 h, which may reflect marginally incomplete *Tau* deletion and is consistent with the shorter ensemble period (Fig. S6F).

To test whether the emergent period of the chimeric SCN was simply the average of all of the individual cellular periods, the SCN

ensemble period before treatment with TTX was compared with the predicted average intrinsic period calculated from the individual cellular periods during TTX. For control WT and *Tau* SCN, these measures were in direct register (Fig. 2B), but this was not the case for the chimeric SCN. The periods of three of four Revertant SCNs and three of three Non-Revertant SCNs fell outside the 95% confidence interval set about the linear regression of the control SCN slices (Fig. 2B). Thus, Revertant SCNs oscillated with a period longer than predicted by their constituent cells, suggesting that the 24-h cells carried more "weight" within the Revertant circuit. Conversely, the Non-Revertant SCNs had a period shorter than predicted, and thus 20-h cells dominated. Furthermore, the mean periods under TTX were comparable between Revertants and Non-Revertants, consistent with them having comparable genetic status (mean ± SEM—Revertants, 22.4 ± 0.40 h; Non-Revertants, 21.5 ± 0.22 h; $n = 4$ and 3; $P = 0.23$, t test). Thus, nonlinear computations based on cell-autonomous periods determined the ensemble period of the SCN. Pace-setting can therefore be unequally weighted in favor of particular cells in the circuit: In the majority of SCNs, it was the *Drd1a* cells, but in Non-Revertant SCNs, the non-*Drd1a* cells held sway. In both cases, the heterochronic circuit was nevertheless synchronized and functional.

Circuit-Level Circadian Pacemaking in Temporally Chimeric SCN. Having confirmed cellular chimerism in the DCR-$CK1\varepsilon^{Tau}$ SCN, we examined the circuit-level behavior by focusing on the wave of PER2::LUC bioluminescence, which follows a stereotypical spatiotemporal orbit across the SCN (Fig. 3A). In CCD time-lapse recordings, this can be described by center-of-mass (CoM) analysis (Fig. 3B) (18). In WT SCN, the CoM followed the trajectory described previously (18–20), sweeping from dorso-medial to ventral SCN and back again. The 20-h *Tau* SCN exhibited comparable geometry in the wave CoM (Fig. 3B). An attractive hypothesis with experimental support is that the leading edge of the wave arises in the dorsomedial SCN because cells in this region have a shorter cell-autonomous period (8, 21). In the chimeric SCN, short-period (20 h) DCR⁻ cells are distributed predominantly in the central SCN, not the dorsomedial SCN, and so if this hypothesis were correct, the geometry of the wave should be different. In both Revertant and Non-Revertant SCNs, however, the geometry and path lengths of the trajectories of the wave CoM were comparable to control slices (Fig. 3 B and C). Chimerism did not, therefore, affect this higher level organization of circadian timekeeping: circuit-based mechanisms were able to impose a common, stereotypical spatiotemporal order even though the mix of cell-autonomous and ensemble periods was different between SCNs. Thus, the wave is not a product of the relative mix of cell-autonomous periods.

Temporal Chimerism in the SCN Confers Plasticity to Behavioral Circadian Rhythms in Mice. In Mixed-period mice, the behavioral period changed spontaneously. To test whether the computation of the ensemble period could be systematically reprogramed, WT, *Tau*, and Revertant mice were held on 24-h 12 L:12 D or 20-h 10 L:10 D lighting schedules before transfer to continuous dim red light (continuous darkness, DD). As noted earlier, both WT and Revertant mice entrained very effectively to the 24-h cycle (Fig. 4A and Fig. S7A), whereas *Tau* mice did not, and on transfer to DD, all groups exhibited their intrinsic periods (Fig. 4A and Fig. S7B). Conversely, *Tau* but not WT mice were able to entrain to the 20-h cycle (Fig. S6 C and D). Unexpectedly, Revertant mice were also able to express stable 20-h behavioral rhythms on the 20-h lighting cycle (Fig. 4A). Furthermore, on transfer to DD, they had a period close to 20 h (Fig. 4 D and E), whereas WT mice instead ran at ca. 24 h. The exposure to a 20-h lighting cycle had therefore brought about a long-term reprogramming of the chimeric SCN, enabling it to sustain a 20-h period. This unanticipated flexibility of period-setting is
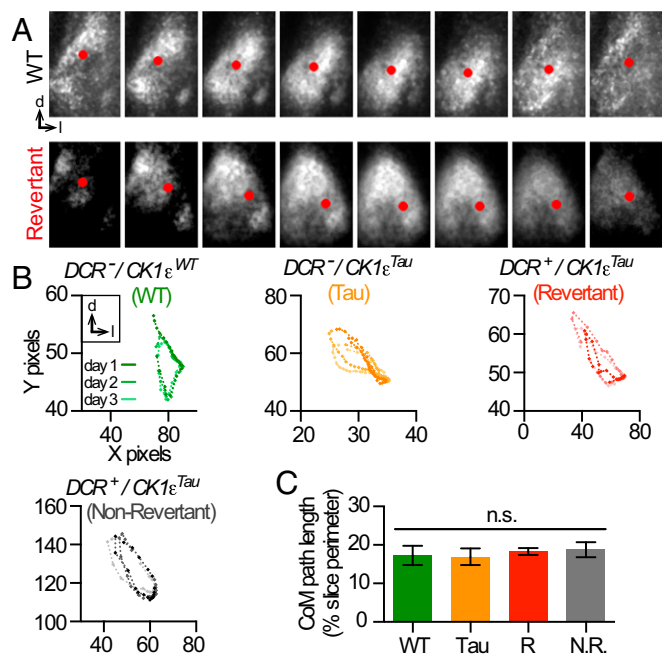

Fig. 3. Spatiotemporal waves of circadian PER2::LUC bioluminescence are conserved in temporally chimeric SCN. (A) Frames from representative CCD recordings of WT and Revertant SCNs to illustrate wave-like dorso-medial to ventral-lateral movement of CoM of bioluminescence (red dot). (B) Poincaré plots of circadian CoM wave trajectory over 3 d (dark-, medium-, and light-colored lines for each consecutive day) from representative control WT and *Tau*, and Revertant and Non-Revertant temporally chimeric SCNs. (C) Group data ($n \geq 3$, mean ± SEM) illustrate path length of CoM trajectory. The extent of the spatiotemporal wave in the DCR⁺ chimeric SCN, for both Revertant (R) and Non-Revertant (NR) SCN, is not significantly different from control WT and *Tau* SCN (one-way ANOVA, $P = 0.89$).

inconsistent with any change in Cre-mediated excision and must reflect reorganized circuit-level computations.

To determine the origin of this 20-h period, SCNs were dissected from mice that had previously entrained to either a 20-h or 24-h LD cycle (Fig. 4C). Slices taken from mice kept on a 24-h cycle all maintained their respective intrinsic periods in culture (Fig. 4D). This was also the case for SCN slices taken from mutant *Tau* and WT animals kept on a 20-h cycle, where WT SCNs reverted to a ca. 24-h period after the first cycle (Fig. 4D and Fig. S7E). This, however, was not the case for the SCN of chimeric mice. For the first 3 d in culture, the SCN oscillated with a period close to 20 h, and then the period lengthened progressively to ca. 24 h by the sixth cycle (Fig. 4D and Fig. S7F). It should also be noted that the rhythms were very unstable during this adjustment phase, where there were large fluctuations of period, before settling down to 24 h (Fig. 4 C and D). In conclusion, the 20-h LD cycle reprogrammed the computation of behavioral and SCN periods of temporally chimeric animals. This recomputation was stable in DD, but once the SCN was isolated in culture, it progressively reverted to its earlier 24-h period. Thus, even though under steady-state conditions the circuit-level specification of circadian period is stable and self-organizing, appropriate retinal activation of the SCN can reversibly alter the computation of the ensemble period and reconfigure the circuit and its control over circadian behavior.

Discussion

To explore how cell-autonomous properties relate to circuit-level circadian functions of the SCN, we created DCR-$CK1\varepsilon^{Tau}$ temporally chimeric mice, which contained a neurochemically and functionally distinct subpopulation of *Drd1a* cells with a 24-h period, alongside non-*Drd1a* cells with a 20-h period. This revealed a series
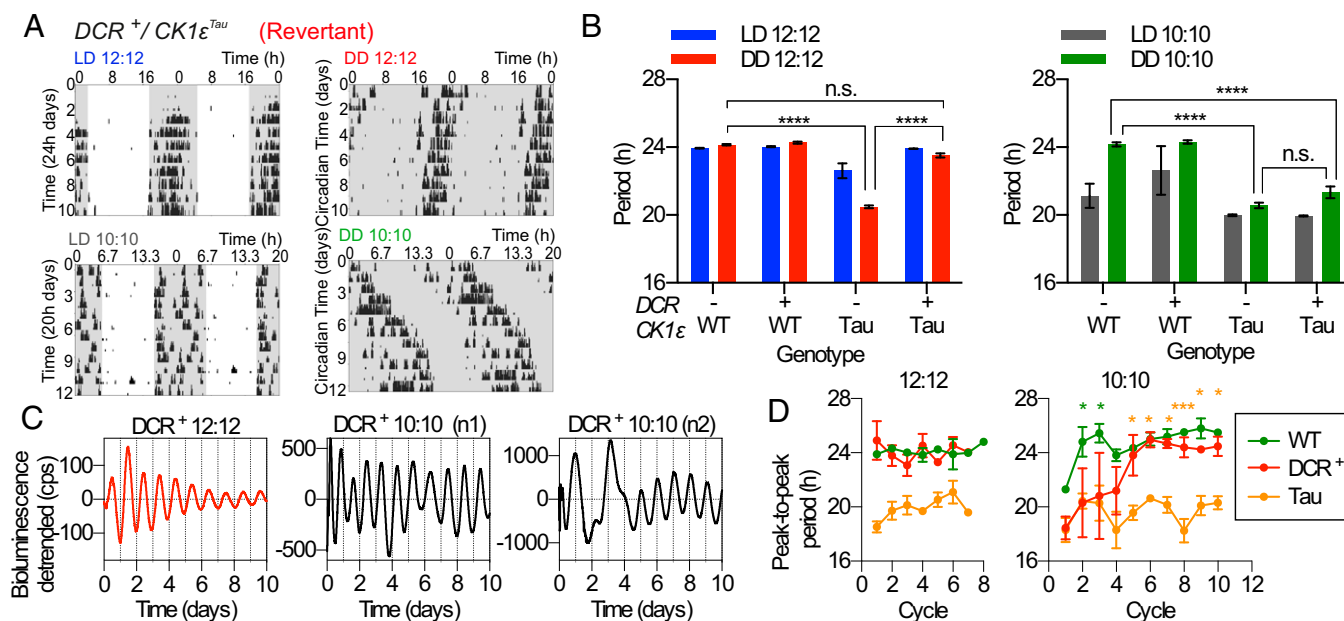
Fig. 4. Photic reprogramming of the circadian period in Revertant temporally chimeric mice. (*A*) Representative, double-plotted actograms for a Revertant mouse subjected to different lighting schedules. The mouse was exposed to a LD 12:12 schedule (*Top Left*) and then transferred to DD (*Top Right*), both plotted on a 24-h time base. The mouse was then exposed to LD 10:10 (*Bottom Left*) and then transferred to DD (*Bottom Right*), both plotted on a 20-h time base. (*B*) Period of wheel-running rhythm (group mean + SEM) under LD 12:12, succeeding DD (*Left*) and LD 10:10, succeeding DD (*Right*). When kept in LD 12:12, chimeric mice subsequently had a mean period not different from WT ($P = 0.40$), but after LD 10:10, they were then not significantly different from *Tau* mice ($P = 0.24$). Periods for WT and *Tau* mice were significantly different from each other after both lighting schedules (two-way ANOVA, ****$P < 0.0001$ by Tukey's comparison). (*C*) PER2::LUC bioluminescence traces (de-trended) from representative Revertant SCNs from animals kept in LD 12:12 (red) or LD 10:10 (black), immediately before slice preparation and recording. (*D*) Group data ($n = 4$ per group, mean ± SEM) of peak-to-peak period of each cycle for SCNs from animals kept in LD 12:12 or LD 10:10. Note the trend for period increase in the Revertant SCNs from LD 10:10 mice but no change in Revertant SCNs from LD 12:12 mice. Revertant animals had significantly shorter periods than WT at the start of the recordings (green; *$P < 0.05$) but then significantly longer periods than *Tau* animals after the fifth cycle (two-way ANOVA with Tukey's comparison; orange; *$P < 0.05$, ***$P < 0.001$).

of circuit-level operating principles of the SCN. First, synchrony and a common period can be imposed on a temporally heterogeneous population of cells: marked divergence of cell-autonomous periods did not disable the circuit. Second, determination of the ensemble circadian period of the SCN is a nonlinear computation, rather than simple averaging. Third, spatiotemporal waves of circadian gene expression are generated by circuit-level mechanisms indifferent to contrasting cell-autonomous periods. Finally, circadian period-setting is flexible, such that under particular circumstances *Drd1a* or non-*Drd1a* cells can set the ensemble period and that this relative dominance can be reversibly reprogrammed by the LD cycle.

The Revertant phenotype demonstrated that targeting a neuronal subpopulation in an otherwise competent SCN circuit could dramatically alter the circadian period of the entire animal. Hence, 24-h *Drd1a* cells dominated the 20-h non-*Drd1a* cells. Similar pace-setting effects have been reported for AVP cells in *AVP-Bmal*$^{-/-}$ mice (14) and for neuromedin-S (NMS) cells in *NMS-Clock*^{delta19} mice (15), although the effects on period were less pronounced (<1 h) than with *DCR-CK1ε*^{Tau} mice. The effects seen in *AVP-Bmal*$^{-/-}$ mice likely arose from localized loss of neuropeptide expression and thus disruption and loosening of circuit-level coupling. The SCN of *DCR-CK1ε*^{Tau} mice had normal neuropeptide expression, and so period effects arose in the presence of effective coupling. Interestingly, expression of *Clock*^{delta19} solely in VIP neurons did not affect in vivo period (15). Given that essentially all AVP neurons are NMS$^+$ (15), the simplest interpretation is that AVP cells alongside non-VIP *Drd1a* cells and perhaps unidentified, non-VIP, NMS$^+$ cells form the top level of a pace-setting hierarchy (Fig. S8).

Pace-setting is clearly not an absolute cellular property, however. Rather, it reflects the circuit context: Non-*Drd1a* cells dominated in Non-Revertant animals. Moreover, Mixed-period mice showed regular transitions between long and short behavioral periods. The

origin of the period spectrum is unclear. We found no evidence of a genetic cause: transgene copy number, EYFP-reported Cre activity in the SCN, and deletion efficiency did not differ between mice of contrasting phenotypes. We cannot exclude, however, the possibility of subtle variability in the efficacy of *Tau* excision, and indeed single-cell analysis highlighted a trend for fewer cells of longer period in Non-Revertant SCNs. Several lines of evidence argue, however, for a circuit-level, nongenetic origin to the spectrum. First, Mixed-period mice showed spontaneous changes of behavioral period from short to long and long to short. The latter is incompatible with a genetic model: excision of the *Tau* allele is irreversible. Second, Revertant mice exhibited unanticipated plasticity of period in response to nonresonant lighting cycles. Again, conversion from a long to short period is incompatible with a genetic, excision-based model. Finally, in both Revertant and Non-Revertant SCNs, single-cell analysis under TTX showed that the computation of ensemble period of an intact circuit, irrespective of its absolute value, was nonlinear. Thus, pace-setting may not be based on irreversible cellular identities but instead based on complex and flexible computations (22). The power of these computations is revealed by the surprising robustness within the SCN, which incorporated a wide range of cell-intrinsic periods into a functional and synchronous circuit. Theoretical data from a generic, coupled-oscillator mathematical model (23) and experimental data from the *Clock*^{delta19} chimera mouse (24) support a linear computation model of ensemble period. These studies, however, involved a random, evenly distributed mixture of WT and mutant cells that do not consider cellular heterogeneity. Here we specifically targeted the *Drd1a* cells, and consistent with some formal models (25), our results support hierarchical, nonlinear period determination within the SCN, with the *Drd1a* intrinsic period dominating pace-setting in the majority of cases. Thus, circuit-level mechanisms, likely neuropeptidergic (9), can override the genetically

specified period of subordinate SCN cells when they are embedded in a fully functional circuit.

Contrary to previous speculation that the spatiotemporal wave arises through short-period cell phase leading (8, 21), our results show that this is not the case. The chimeric SCN exhibited comparable wave geometry, despite having a very different spatial mapping of intrinsic circadian periods. Thus, the wave is generated by circuit-level mechanisms indifferent to contrasting cell-autonomous periods. Peptidergic control is likely a key component of its generation: For example, chemogenetic activation of VIP cells can reprogram the wave (18).

Finally, the retinally mediated reprogramming of the behavioral period has echoes of the "aftereffects" described in classical circadian biology, where non–24-h lighting regimes can modulate period. In WT mice (26, 27), these effects are small (<1 h), whereas the behavioral periods of chimeric mice were reprogrammed by 2.2 ± 0.3 h. This recoding was an intrinsic property of the SCN because immediately on recording, SCNs from Revertant animals exposed to 20-h LD had a short period. This was not sustained, however, and the period lengthened progressively over 3–4 d, "relaxing" back to 24 h. Similar relaxation is seen in the SCNs of animals exposed to "long day" photoperiodic cycles (20 L:4 D), where phase-splitting in PER2 rhythms of core and shell regions gradually resynchronized in vitro (19). Our data not only show that photic input to the SCN can alter the relative contributions of *Drd1a* and non-*Drd1a* cells to the computation of ensemble period, but also they present the possibility that extra-SCN signals are required to sustain this new program in vivo. SCN grafting studies (9) suggest that even though SCN slices do not capture all SCN neurons, sufficient network communication is present to support reprogramming in vitro. A potential origin of extra-SCN signals is the retina: retinal innervation is necessary to sustain a circadian rhythm of MAP kinase activity restricted to the SCN core of hamsters (28). Although the retina does not normally affect circadian pacemaking, it has a clock. We hypothesize that non-*Drd1a* cells in the retinorecipient core of the SCN, such as GRP neurons, could acquire dominance under 20-h LD conditions through resonance with the photic cues from the 20-h retina, whereas 24-h VIP cells receive heterochronic stimulation on a 20-h schedule and so lose coherence. In contrast, once the slice is made, this direct, resonant stimulation is lost, and progressively, the 24-h cells in the circuit come to dictate period.

In conclusion, we have demonstrated an unanticipated flexibility in the determination of ensemble period, providing a new perspective on the concept of pacemaker cells in the SCN. Moreover, we have revealed a series of operating principles that govern the interactions between cell-autonomous and circuit-level functions of the SCN. Elucidation of the mechanisms that implement these principles offers an opportunity to understand how cell interactions support neuronal computations to generate flexible emergent programs of behavior. This has strong parallels with studies in *Drosophila*, where genetic manipulation of kinase or TTFL components in subgroups of fly neurons can impose particular cell-autonomous periods over the circuit and behavior (29). The fly circuit does not, therefore, operate in a simple linear manner. The logic of circadian computations may therefore be a conserved feature of flies and mammals.

Materials and Methods

Animal work was conducted in accordance with the UK Animals (Scientific Procedures) Act 1986, with Medical Research Council Laboratory of Molecular Biology Local Ethical Review Committee. Wheel-running patterns were analyzed using ClockLab (ActiMetrix Inc.). SCN and peripheral tissue slices were prepared as previously described (30). Bioluminescence emission was recorded using photon multipliers (Hamamatsu), CCD cameras (Hamamatsu), or LV200 bioluminescence imaging systems (Olympus). Graphs were plotted, data analyses performed, and statistical tests calculated using Prism 6 (GraphPad). A more detailed description of the materials and methods are provided in *SI Materials and Methods*.

1. Mohawk JA, Takahashi JS (2011) Cell autonomy and synchrony of suprachiasmatic nucleus circadian oscillators. *Trends Neurosci* 34(7):349–358.
2. Asher G, Schibler U (2011) Crosstalk between components of circadian and metabolic cycles in mammals. *Cell Metab* 13(2):125–137.
3. Chen SK, Badea TC, Hattar S (2011) Photoentrainment and pupillary light reflex are mediated by distinct populations of ipRGCs. *Nature* 476(7358):92–95.
4. Viswanathan N, Weaver DR, Reppert SM, Davis FC (1994) Entrainment of the fetal hamster circadian pacemaker by prenatal injections of the dopamine agonist SKF 38393. *J Neurosci* 14(9):5393–5398.
5. Reppert SM, Weaver DR (2002) Coordination of circadian timing in mammals. *Nature* 418(6901):935–941.
6. Hastings MH, Brancaccio M, Maywood ES (2014) Circadian pacemaking in cells and circuits of the suprachiasmatic nucleus. *J Neuroendocrinol* 26(1):2–10.
7. Liu AC, et al. (2007) Intercellular coupling confers robustness against mutations in the SCN circadian clock network. *Cell* 129(3):605–616.
8. Yamaguchi S, et al. (2003) Synchronization of cellular clocks in the suprachiasmatic nucleus. *Science* 302(5649):1408–1412.
9. Maywood ES, Chesham JE, O'Brien JA, Hastings MH (2011) A diversity of paracrine signals sustains molecular circadian cycling in suprachiasmatic nucleus circuits. *Proc Natl Acad Sci USA* 108(34):14306–14311.
10. Maywood ES, et al. (2013) Analysis of core circadian feedback loop in suprachiasmatic nucleus of mCry1-luc transgenic reporter mouse. *Proc Natl Acad Sci USA* 110(23):9547–9552.
11. Heintz N (2004) Gene expression nervous system atlas (GENSAT). *Nat Neurosci* 7(5):483.
12. Meng QJ, et al. (2008) Setting clock speed in mammals: The CK1 epsilon tau mutation in mice accelerates circadian pacemakers by selectively destabilizing PERIOD proteins. *Neuron* 58(1):78–88.
13. Husse J, Zhou X, Shostak A, Oster H, Eichele G (2011) Synaptotagmin10-Cre, a driver to disrupt clock genes in the SCN. *J Biol Rhythms* 26(5):379–389.
14. Mieda M, et al. (2015) Cellular clocks in AVP neurons of the SCN are critical for interneuronal coupling regulating circadian behavior rhythm. *Neuron* 85(5):1103–1116.
15. Lee IT, et al. (2015) Neuromedin s-producing neurons act as essential pacemakers in the suprachiasmatic nucleus to couple clock neurons and dictate circadian rhythms. *Neuron* 85(5):1086–1102.
16. Srinivas S, et al. (2001) Cre reporter strains produced by targeted insertion of EYFP and ECFP into the ROSA26 locus. *BMC Dev Biol* 1:4.
17. Yoo SH, et al. (2004) PERIOD2:LUCIFERASE real-time reporting of circadian dynamics reveals persistent circadian oscillations in mouse peripheral tissues. *Proc Natl Acad Sci USA* 101(15):5339–5346.
18. Brancaccio M, Maywood ES, Chesham JE, Loudon AS, Hastings MH (2013) A Gq-Ca2+ axis controls circuit-level encoding of circadian time in the suprachiasmatic nucleus. *Neuron* 78(4):714–728.
19. Evans JA, Leise TL, Castanon-Cervantes O, Davidson AJ (2013) Dynamic interactions mediated by nonredundant signaling mechanisms couple circadian clock neurons. *Neuron* 80(4):973–983.
20. Yamaguchi Y, et al. (2013) Mice genetically deficient in vasopressin V1a and V1b receptors are resistant to jet lag. *Science* 342(6154):85–90.
21. Doi M, et al. (2011) Circadian regulation of intracellular G-protein signalling mediates intercellular synchrony and rhythmicity in the suprachiasmatic nucleus. *Nat Commun* 2:327.
22. Abrahamson EE, Moore RY (2001) Suprachiasmatic nucleus in the mouse: Retinal innervation, intrinsic organization and efferent projections. *Brain Res* 916(1-2):172–191.
23. Abraham U, et al. (2010) Coupling governs entrainment range of circadian clocks. *Mol Syst Biol* 6:438.
24. Low-Zeddies SS, Takahashi JS (2001) Chimera analysis of the Clock mutation in mice shows that complex cellular integration determines circadian behavior. *Cell* 105(1):25–42.
25. Bernard S, Gonze D, Cajavec B, Herzel H, Kramer A (2007) Synchronization-induced rhythmicity of circadian oscillators in the suprachiasmatic nucleus. *PLOS Comput Biol* 3(4):e68.
26. Aton SJ, Block GD, Tei H, Yamazaki S, Herzog ED (2004) Plasticity of circadian behavior and the suprachiasmatic nucleus following exposure to non-24-hour light cycles. *J Biol Rhythms* 19(3):198–207.
27. Azzi A, et al. (2014) Circadian behavior is light-reprogrammed by plastic DNA methylation. *Nat Neurosci* 17(3):377–382.
28. Lee HS, Nelms JL, Nguyen M, Silver R, Lehman MN (2003) The eye is necessary for a circadian rhythm in the suprachiasmatic nucleus. *Nat Neurosci* 6(2):111–112.
29. Yao Z, Shafer OT (2014) The Drosophila circadian clock is a variably coupled network of multiple peptidergic units. *Science* 343(6178):1516–1520.
30. Hastings MH, Reddy AB, McMahon DG, Maywood ES (2005) Analysis of circadian mechanisms in the suprachiasmatic nucleus by transgenesis and biolistic transfection. *Methods Enzymol* 393:579–592.